Proceedings of the 6th International Conference on Gas Hydrates (ICGH 2008),
Vancouver, British Columbia, CANADA, July 6-10, 2008.

EFFECT OF GRAIN CHARACTERISTICS ON THE BEHAVIOUR OF DISSEMINATED METHANE HYDRATE BEARING SEDIMENTS

Emily Kingston[1,*], Chris Clayton[1], Jeffery Priest[1] and Angus Best[2]

[1]School of Civil Engineering and the Environment
University of Southampton
Highfield, Southampton, SO17 1BJ
UNITED KINGDOM

[2]Southampton Oceanography Centre,
European Way, Southampton, SO14 3ZH
UNITED KINGDOM

ABSTRACT

Results of seismic surveys are routinely used to assess the presence of methane hydrate in deep ocean sediments. Accurate estimates of hydrate distribution and volume within the sediment are required to assess the potential of gas hydrate as an energy resource, driver for climate change or as a geotechnical hazard. However, seismic velocity may be affected not only by the quantity and morphology of the hydrate, but also by the properties of the host sediment, for example its particle size distribution and grain shape. This paper reports the results of experiments conducted to determine dynamic geophysical properties such as compressional wave velocity (V_p), shear wave velocity (V_s) and their respective attenuation measurements (Q_p^{-1} and Q_s^{-1}) of specimens with varying amounts of disseminated methane hydrate within materials with different particle shapes and sizes. The results show that the impact of disseminated hydrate is affected both by mean particle size and by particle sphericity, with the surface area of the sediment grains influencing the spread of hydrate throughout a material and therefore it's bonding capabilities. The sediments with 10% hydrate content show the highest surface areas correspond to the least increase in seismic velocity while sediments with low surface areas gives the most.

Keywords: bonding, grain size, grain shape, disseminated hydrate

NOMENCLATURE

Q_s^{-1}	Shear wave attenuation
Q_p^{-1}	P- wave attenuation
Q_{lf}^{-1}	Longitudinal was attenuation
V_s	Shear wave velocity (ms^{-1})
V_p	P- wave velocity (ms^{-1})
V_{lf}	Longitudinal wave velocity (ms^{-1})
σ'	isotropic effective stress

INTRODUCTION

The behaviour of granular soils is known to be influenced by characteristics of the soil such as particle size and the distribution of particle sizes making up the soil as well as attributes of the particles such as shape, roundness, surface roughness and specific gravity [1, 2]. Studies have shown that the mechanical properties of a sand can be altered, from a dilative behaviour to a contractive behaviour, due to the introduction of finer grained particles of varying shapes [3, 4]. The effect that gas hydrate may have on these soils must be evaluated to improve our understanding of results from seismic surveys conducted on natural hydrate bearing sediments.

* Corresponding author: Phone: +44 2380 595439 Fax +44 2380 677519 E-mail: evlk@soton.ac.uk

Previous studies into the impact of gas hydrates within the laboratory have mainly focused on soils with a uniform particle size and shape [5-9]. This research presents the results from tests on soils of varying particle size, distribution and shape for a given hydrate content. The aim is to highlight the influence these factors have on the way hydrate changes the properties of the host material.

APPARATUS AND METHODOLOGY

The Gas Hydrate Resonant Column (GHRC) simulates the pressure and temperature conditions necessary for gas hydrate formation in the laboratory. A maximum pressure of 25MPa can be applied to a cylindrical 70mm diameter specimen, with temperature control from -20°C to 50°C. A full description of the GHRC and its development can be found in Clayton *et al***.** [10].

Materials Tested

A number of granular materials were chosen for a set of tests that would investigate the effect of hydrate on sediments with varying grain size and shape. The materials chosen were Leighton Buzzard sand grade B (LBB), Leighton Buzzard sand grade E (LBE) and 100 mesh muscovite mica (mica). The properties of each material are shown in Table 1. Leighton Buzzard sand is a natural, uncrushed silica sand that is free from silt, clay or organic matter (Figures 1 and 2). The muscovite mica used in these tests has the same grain size as the grade E sand. However, mica is a platy material and so gives a variety in particle shape (Figure 3).

The addition of fines to a rotund material will alter it's behaviour depending on the fines content. 20% fines by weight will dominate the behaviour of a rotund sand, so some material mixes used in this research set with a 10% fines content so as to maximize surface area influences without dominating material behaviour. Four different specimen mixtures were used for testing:

- Leighton Buzzard grade B sand (LBB)
- Leighton Buzzard grade E sand (LBE)
- Leighton Buzzard grade B sand mixed with 10% by weight Leighton Buzzard grade E sand (LBB/LBE)
- Leighton Buzzard grade B sand mixed with 10% by weight muscovite mica (LBB/mica).

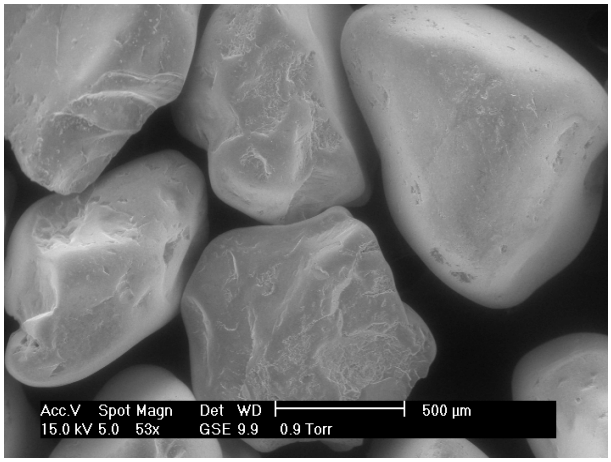

Figure 1 Scanning electron micrograph of Leighton Buzzard sand grade B

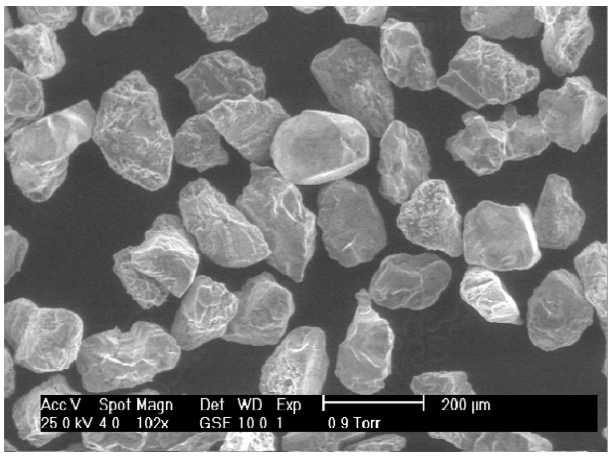

Figure 2 Scanning electron micrograph of Leighton Buzzard sand grade E.

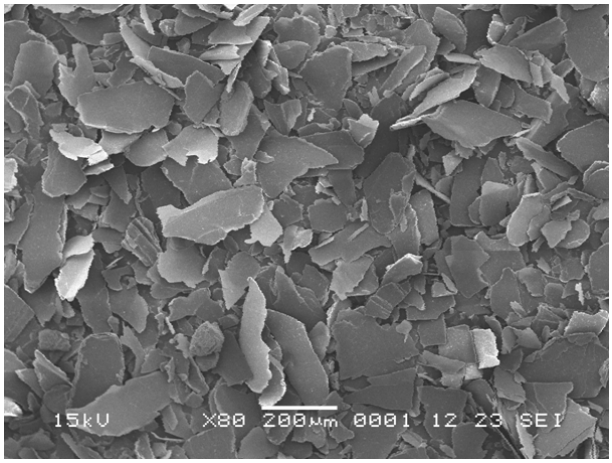

Figure 3 Scanning electron micrograph of 100 mesh mica

Initial resonant column tests were conducted on each of these mixtures with no hydrate in the pore space, in order to measure their basic behaviour.

Specimen Preparation

The method of hydrate formation adopted in this testing sequence was that of Waite *et al*. [8] and Priest *et al*. [11], where hydrate is made in partially saturated conditions. Hydrate content is controlled by the quantity of water added in the pore space of the specimen, with methane being fed into the pore space at constant pressure (the "back pressure").

	Leighton Buzzard Sand B	Leighton Buzzard Sand E	Mica 100 Mesh
Particle size	1.18 – 0.6mm	90-150µm	52-105µm
Particle shape	Rounded – Sub-rounded	Rounded – Sub-rounded	Flat, platy
Specific Gravity	2.65	2.65	2.90
Max. dry density	1752kgm^{-3}	1624kgm^{-3}	912kgm^{-3}
Min. dry density	1496kgm^{-3}	1331kgm^{-3}	728kgm^{-3}

Table 1 Properties of the materials used in GHRC testing. From Clayton *et al*. [10] and Theron [12].

The target hydrate content for each specimen was selected to be 10% of the volume of the pore space. This value was chosen because previous experiments by Priest et al. [11] on LBE sand, using varying quantities of hydrate, had suggested (Figure 4) that at hydrate contents greater than 5% full bonding occurred. The uncemented grains have a seismic velocity that is strongly dependant on effective stress. Fitting the relationship $Vs = A\sigma'^{b}$ to the curve of seismic velocity as a function of effective stress, σ', gives an exponent (b) value of 0.25. Bonding progressively decreases the influence of effective stress, with b approaching zero as full cementing occurs.

The required quantity of water needed for each sediment type was calculated from the dry densities of the control tests shown in Table 2, and ranged between 2 and 2.5% total moisture content dependant on soil mixture. The specimens were prepared by taking the required mass of material that would make up a 70mm by 140mm specimen, and mixing it with the correct mass of water (see Table 3 for exact values used). The partially saturated material was then left in a sealed container for 12 hours at room temperature to allow the moisture to distribute itself homogeneously.

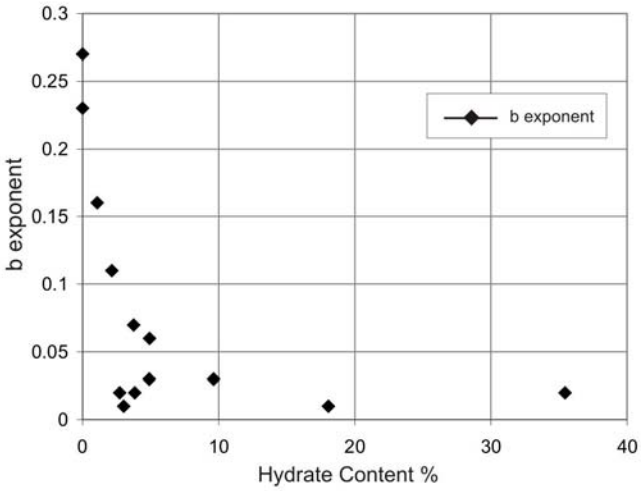

Figure 4 b exponent plotted against hydrate content as a percent of the pore space, for tests conducted on LBE sand. From Priest et al. [11].

Specimen	Mass LB-B (g)	Mass LB-E (g)	Mass Mica (g)	Vol (cm^{-3})	Dry density (kgm^{-3})	Void ratio
LBB-D	940.9			551	1706.2	0.553
LBE-D		800.7		517	1548.1	0.712
LBB/LBE-D	883.7	101.2		546	1804.3	0.469
LBB/Mica-D	870.7		98.3	541	1792.4	0.492

Table 2 Dry densities and void ratios of dry specimens produced for control tests (0% hydrate)

Specimen	Water Content (%)	Dry density (kgm^{-3})	Void ratio
LBB-H	2.29	1662.5	0.595
LBE-H	2.49	1505.5	0.760
LBB/LBE-H	1.93	1708.1	0.543
LBB/Mica-H	2.33	1676.0	0.592

Table 3 Basic properties of the specimens used in the hydrate tests (10% hydrate)

Specimens were formed by the moist tamping technique [13]. This method allows for dense specimens to be made by packing the sediment/water mixture into a split mould in 12-15 equal layers, with each layer tamped with a rubber bung. Once the specimen was at full height (nominally 140mm) the leftover sediment/water mixture was weighed, dried and sieved to determine the masses of each material in the specimen.

Once the specimens were formed in the split mould, the top cap was attached, and a vacuum of ~50kPa was applied to allow for removal of the mould. The drive mechanism could then be attached to the specimen, with thermistors and an LVDT also attached to monitor temperature and height changes respectively. A confining pressure of 250kPa was then applied using nitrogen gas.

The specimens were taken into the hydrate stability region by first increasing the back pressure of the system to 15MPa by the injection of methane gas (points A to B in Figure 4). The external cell pressure tracked the increase in back pressure so that an isotropic effective stress of 250kPa was maintained on the specimen at all times. The temperature of the system was then reduced to 2°C to initiate hydrate formation (point C in Figure 4). During the temperature drop and subsequent hydrate formation, the cell and back pressures were maintained at 15.25MPa and 15MPa respectively. Each specimen was held under these conditions for 24 hours, at which point all hydrate was considered to have formed. Clayton et al. [10] suggest a minimum of 15 hours for hydrate formation in these conditions.

Resonant Column Testing

The seismic velocities V_s and V_p, and associated attenuation (Q_s^{-1} and Q_p^{-1} respectively) are calculated from the resonant frequency of the specimen during testing with the GHRC. The specimen is excited in either torsional or flexural vibration through a range of applied frequencies. An accelerometer mounted on the top cap measures the amplitude of vibration of the system, with the resonant frequency being defined when the output from the accelerometer is a maximum. Shear wave velocity V_s is derived through torsional excitation, whereas longitudinal wave velocity V_{lf}, and from this P-wave velocity V_p is found through flexural excitation. Attenuation in these tests was measured by the free vibration decay (FVD) method. Details on the full data reduction for torsional and flexural excitation, and attenuation measurements, can be found in Priest *et al.* [11, 14].

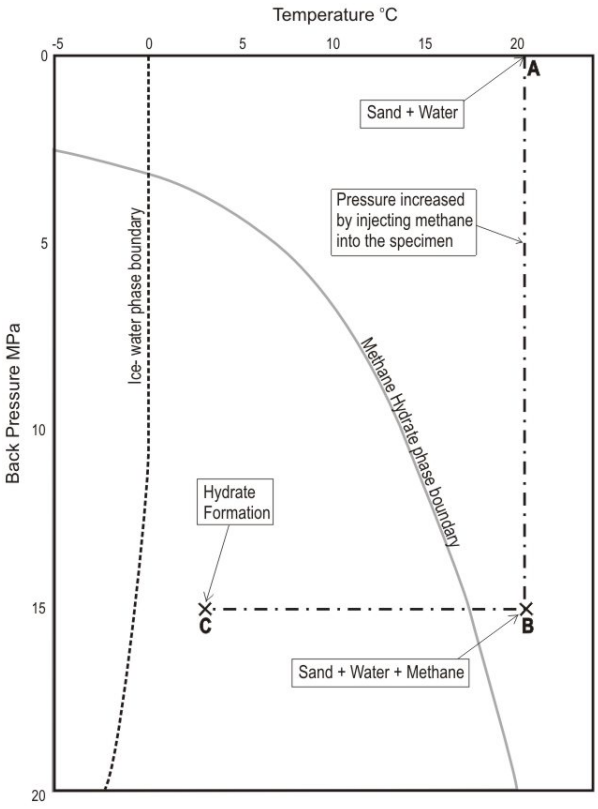

Figure 5 Plan of the route taken for each of the different sediment tests into the hydrate stability zone (also marked).

Resonant column tests were conducted at a range of effective stresses; 250, 500, 750, 1000, 1500 and 2000kPa, with each load step held for 30 minutes before testing. Once the maximum effective stress was achieved, the load sequence was reversed and the specimen returned to it's initial stress state. Torsional and flexural resonant frequencies and associated attenuation measurements were recorded at each step.

RESULTS AND DISCUSSION

A total of 8 tests were conducted. Each sediment type was tested with 0 % and 10 % hydrate content in the pore space. Figure 6 shows shear wave velocity, V_s, for each sediment with and without

hydrate, plotted against effective confining pressure σ'. The results show that the inclusion of 10% hydrate in the pore space greatly increases the shear wave velocity of all the specimens, although to different degrees. The difference between the velocities for the non-hydrated specimens and those specimens containing 10% hydrate in the pore space are plotted in Figure 8.

As mentioned above, previous work on LBE sand containing methane gas hydrate [11] has shown that hydrate fully bonds the sand after about 5% of the pore space is filled with hydrate under these partially saturated conditions. In the specimens tested in this research, 10% hydrate content in the pore space was sufficient to bond each type of specimen mixture, with the b exponent values falling to around the values shown in Figure 4 for 10% hydrate content (Table 4).

	A constant	b exponent
LBB	1161	0.0305
LBE	1024	0.0273
LBB/LBE	1261	0.0180
LBB/mica	1008	0.0266

Table 4 A and b constants for each specimen.

Hydrate can form in three locations in a sediment: on the grain surfaces; at grain contacts; and in the voids between grains (Figure 7). In partially saturated conditions, hydrates form at particle surfaces and contacts where the water resides [8, 10]. The volume of water added to a specimen will be adsorbed on to the mineral surface and then excess water will form at the particle contacts due to capillary action between the grains. The volume of water adsorbed onto grain surfaces in the specimens is directly related to the surface area of the grains available. The materials used in these tests each have a different surface area per grain. In order to estimate the total surface area in each specimen, the grains were approximated as smooth scalene ellipsoids [15], with the surface areas for LBB, LBE and Mica grains being 2.20 x 10^{-6}, 1.52 x 10^{-8} and 1.29 x 10^{-8}m^2 respectively. By also knowing the volume of each scalene ellipsoid grain, the total surface area for the volume of material in each of the specimens could be calculated, and is given in Table 5.

When comparing the values from Table 5 with the results in Figure 8, it seems that the specimens with the smallest surface area, LBB and LBB/LBE, correspond to the specimens that show the largest increase in shear wave velocity when hydrate is formed. The specimens with greater surface area – LBE and LBB/Mica, show a lower rise in shear velocity by the introduction of hydrate into the pore space. This difference, however, is not so great as would be suggested by the calculated differences in surface area.

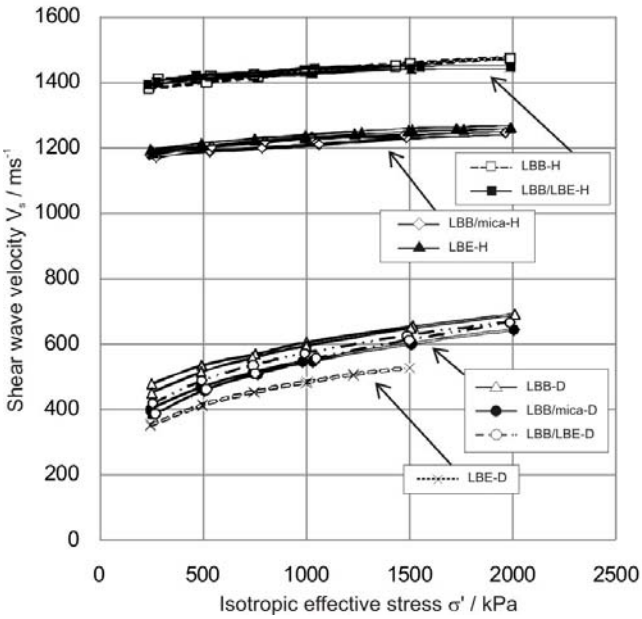

Figure 6 Shear wave velocity V_s against isotropic effective stress σ' for specimen mixture, with and without hydrate in the pore space.

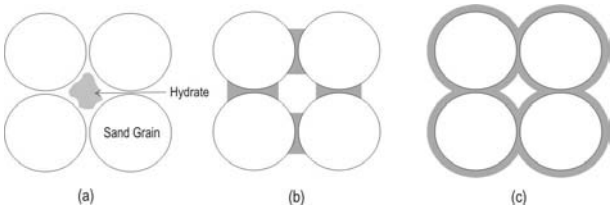

Figure 7 Diagrams showing the possible location of hydrate in a granular material. (a) Hydrate grows in the pore space between the grains. (b) Hydrate forms at grain contacts. (c) Hydrate grows on grain surfaces. Adapted from Dvorkin et al. [16].

Priest *et al*. [11] showed that the seismic velocity, for the LBE sand, increased with increasing quantities of hydrate in the pore space, due to the increase in bonding at particle contacts. Although the volume of added water was calculated to give

the same hydrate content in each specimen, the actual volume of hydrate formed at grain contacts would be reduced to some extent by the surface area of the grains in the specimen. The larger the surface area, more water is required to cover the grain surface, therefore less water will reside at grain contacts, and so give rise to a lower increase in shear wave velocity.

Specimen	Surface area per m^3 of material (m^2)	Surface Area of grains in specimen (m^2)
LBB	8×10^3	2.75
LBE	112×10^3	33.83
LBB/LBE	18×10^3	6.85
LBB/Mica	124×10^3	42.07

Table 5 Estimated surface areas for each specimen, calculated using Thomsen's formulae [17] for the surface area of scalene ellipsoids.

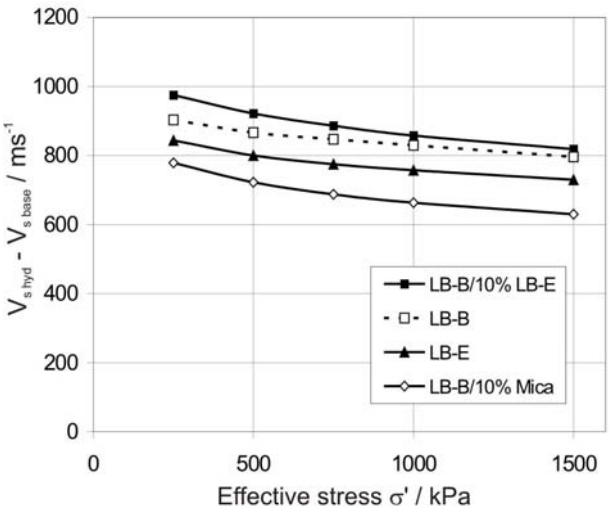

Figure 8 The change in shear wave velocity between hydrated ($V_{s\ hyd}$) and dry ($V_{s\ base}$) specimens for each sediment type, plotted against effective confining pressure σ'.

This hypothesis can be investigated by considering the volume of water bound to grain surfaces. Olhoeft [18] suggests that 7-8 monolayers of water, each 10^{-8}m thick, are bound to silica surfaces in partially saturated rocks. If this value is taken as an average for the grains in our specimens, the volume of water bound on grain surfaces can be calculated. Considering the initial volume of water added to each specimen, the percentage of that water bound to surfaces, for each specimen, is 0.9% for LBB; 2% for LBB/LBE; 12.9% for LBB/mica; and 13.4% for LBE. These values show that the specimens with the smallest surface areas have more water available for bonding at particle contacts than the specimens with a high surface area. The differences in seismic velocities for each specimen, as seen in Figure 8, can therefore be attributed to the different amounts of water residing at grain contacts for bonding.

With material mixes such as those tested here, it is also valuable to consider the direct effect of the range of grain sizes and shapes in each specimen. Research into mixes of granular and platy materials shows that the stiffness of a rotund sand changes with the inclusion of fines [3, 19-21]. It has been shown that introducing mica into a rotund sand reduces the stiffness of that sand by restricting sand-sand grain contacts, and changing the distribution of interparticle forces. Mica will sit in between grains and, if larger enough, bridge over particles and increase material porosity [21]. The 100 mesh mica used in this research is not larger enough to bridge the LBB grains, however it reduces the seismic velocity of the sand by sitting in the pore and between grain contacts, altering the transmission of internal forces [21]. The bonding effect of gas hydrate to a mixture such as this will be reduced in that there is a larger surface area at the grain contacts, and so less hydrate to contribute to bonding.

The addition of small diameter rotund particles to a clean sand of a larger grain size, has less effect on seismic velocity, but alters bulk properties. Table 2 shows the dry densities and void ratios of the dry material mixes, with the LBB/LBE material showing the highest density and lowest void ratio. This is due to the LBE particles lying in the pore spaces, and not interfering with LBB grain contacts [20]. Adding gas hydrate to this material mixture appears to give the largest increase in seismic velocity of all the materials tested (Figure 8). If it is accepted that hydrate acts as a cement in partially saturated conditions, the increased seismic velocity seen in the LBB/LBE mix could be due to the interaction of the hydrate 'cement' with the LBE grains. Cement and concrete research shows that pore filling inclusions to cement mixes increases the cohesive characteristics of concrete [22, 23]. This can be due to an increased number of nucleation and bonding points, or the inclusion of a

solid material in the compliant hydrate cement (Figure 9 a and b).
The nature of gas hydrate in partially saturated environments means that the spread of water throughout a material will dictate the way hydrate affects that material. The estimates of hydrate content in the field from seismic surveys must therefore consider the sediment grain size, distribution and shape, and adjust their estimates for the spread of hydrate over grain surfaces.

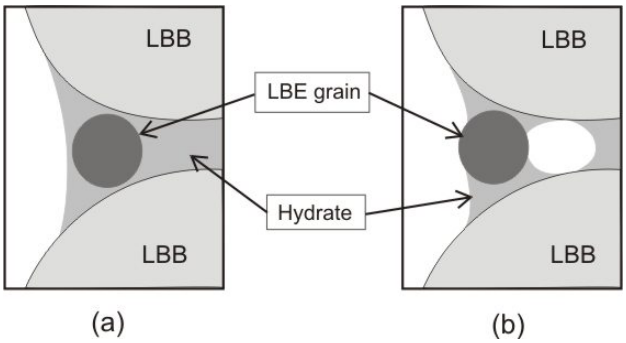

Figure 9 Possible influences of LBE to the cementing effects of hydrate in LBB. (a) LBE contributes to cement at LBB contacts. (b) Cement forms at contacts between LBB and LBE grains as well as at LBB-LBB contacts.

Attenuation

Figure 9 shows the general pattern in attenuation measurements taken for the torsional excitation load cycle. The plot shows that the inclusion of 10% hydrate in the sediment mixtures does not have a significant impact on the attenuation values from the control tests. In near-saturated granular materials, the considered mechanism for energy loss at low strains is through 'squirt flow' [24, 25]. Interstitial water movement contributes to energy dissipation as grain contacts are deformed. The lack of change in attenuation seen in Figure 9 could be attributed to two factors in these tests[14]:

1. The bonded nature of the specimens reduces grain deformation and therefore residual water movement.
2. The formation of hydrate in the pore space has used up any interstitial water so that none is available to contribute to attenuation by the squirt flow mechanism.

Figure 9 also shows the attenuation measurements from a test containing LBE sand and 10% hydrate, but in water saturated conditions (LBE-H saturated). The high attenuation in the saturated test is considered to be due to the squirt flow mechanism. It can be seen that if free water is present, the attenuation of seismic waves is greatly increased in hydrate bearing sediments.

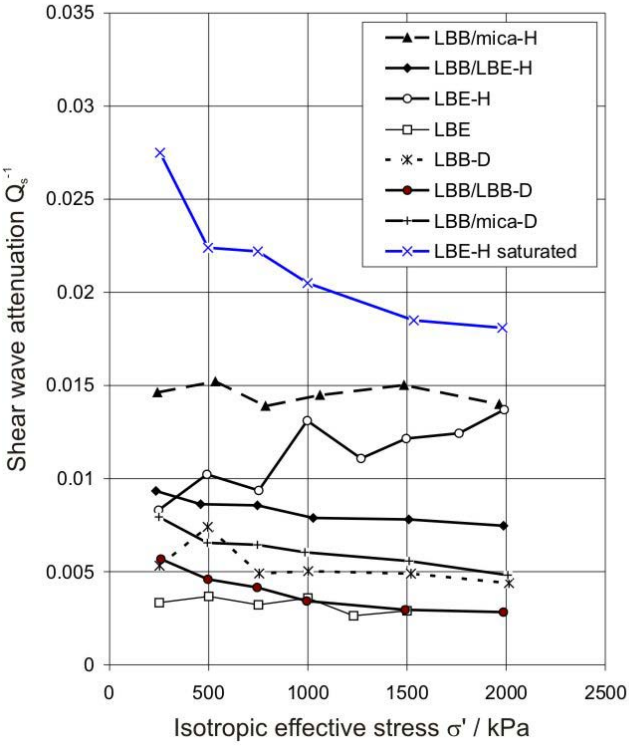

Figure 10 Shear wave attenuation Q_{ls}^{1} plotted against effective confining pressure σ' through the load cycle.

CONCLUSIONS

Methane gas hydrate has been formed in 4 different forms of granular material with varying particle sizes and shapes. Results have shown that an input of 10% hydrate into the pore space causes a strong increase in seismic velocity in all tests, but the degree of change varies for each material type. The surface area of the grains influences the change in mechanical properties caused by hydrate inclusion, with the largest surface areas correlating to the lowest increase in seismic velocity. It can be concluded that due to the morphology of hydrate in partially saturated environments, particle size and shape may have an effect on the way hydrate

bonds a sediment, with the surface area of grains within that sediment playing a secondary role.

Attenuation measurements for each specimen have also been made, and it has been found that attenuation does not increase significantly with the inclusion of 10% hydrate to the pore space. This is thought to be due to the bonding nature of hydrate in partially saturated conditions, and that hydrate formation uses all interstitial water, leaving none to contribute to squirt flow mechanisms.

REFERENCES

[1]. Bolton, M.D., *The strength and dilatency of sands*. Geotechnique, 1986. 36(1): 65-78.

[2]. Mitchell, J.K., *Fundamentals of Soil Behaviour*. 1976, New York: Wiley.

[3]. Clayton, C.R.I., Theron, M., and Vermeulen, N.J. *The effect of perticle shape on the behaviour of gold tailings*. in *Advances in Geotechnical Engineering: The Skempton Conference*. 2004: Thomas Telford.

[4]. Thevanayagam, S., *Effect of fines and confining stress on the un-drained shear strength of a silty sand.* Journal of Geotechnical and Geoenvironmental Engineering, 1998. 124(6): 479-491.

[5]. Berge, L.I., Jacobsen, K.A., and Solstad, A., *Measured acoustic wave velocities of R11 hydrate samples with and without sand as a function of hydrate concentration.* Journal of Geophysical Research, 1999. 104(B7): 15415--15424.

[6]. Buffett, B.A. and Zatsepina, O.Y., *Formation of gas hydrate from dissolved gas in natural porous media.* Marine Geology, 2000. 164: 69--77.

[7]. Stoll, R.D., Ewing, J., and Bryan, G.M., *Anomalous wave velocities in sediments containing gas hydrates.* journal of Geophysical Research, 1971. 76(8): 2090--2094.

[8]. Waite, W.F., Winters, W.J., and Mason, D.H., *Methane hydrate formation in partially saturated Ottawa sand.* American Mineralogist, 2004. 89: 1221--1227.

[9]. Winters, W.J., Dillon, W.P., Pecher, I.A., and Mason, D.H., *GHASTLI--Determining physical properties of sediment containing natural and laboratory formed Gas Hydrate*, in *Natural Gas Hydrate in Oceanic and Permafrost Environments*, M.D. Max, Editor. 2000, Kluwer Academic Publishers: The Netherlands. p. 311--322.

[10]. Clayton, C.R.I., Priest, J.A., and Best, A.I., *The effects of disseminated methane hydrate on the dynamic stiffness and damping of a sand.* Geotechnique, 2005. 55(6): 423--434.

[11]. Priest, J.A., Best, A., and Clayton, C.R.I., *A laboratory investigation into the seismic velocities of methane gas hydrate-bearing sand.* Journal of Geophysical Research, 2005. 110: B04102.

[12]. Theron, M., *The Influence of fine particles on the behaviour of a rotund sand*. 2004, University of Southampton.

[13]. Frost, J.D. and Park, J.-Y., *A critical assessment of the moist tamping technique.* Journal of Geotechnical Testing, 2003. 26(1): 1-14.

[14]. Priest, J.A., Best, A., and Clayton, C.R.I., *Attenuation of seismic waves in methane gas hydrate-bearing sand.* Geophysical Journal International, 2006. 164: 149-159.

[15]. Clayton, C.R.I., Obula Reddy, A.C., and Schiebel, R., *A method of estimating the form of coarse particulates.* Geotechnique, (under review).

[16]. Dvorkin, J., Helgerud, M.B., Waite, W.F., Kirby, S.H., and Nur, A., *Introduction to physical properties and Elasticity models*, in *Natural Gas Hydrate in Oceanic and Permafrost Environments*, M.D. Max, Editor. 2000, Kluwer Academic Publishers: The Netherlands. p. 245--260.

[17]. Thomsen, K. 2004 [cited; Available from: http://home.att.net/~numericana/answer/ellipsoid.htm#thomsen.

[18]. Olhoeft, G.R. *Electrical properties of rocks*. in *The Physics and Chemistry of Rocks and Minerals*. 1976: Wiley.

[19]. Georgiannou, V.N., *Micaceous sands: stress-strain behaviour and the influence of initial fabric*, in *Advanced Laboratory Stress-Strain Testing of*

Geomaterials, F. Tatsuoka, S. Shibuya, and R. Kuwano, Editors. 2001, A A Balkema Publishers: Tokyo. p. 227-235.

[20]. Georgiannou, V.N., *The undrained response of sands with additions of particles of various shapes and sizes.* Geotechnique, 2006. 56(9): 639-649.

[21]. Lee, J.S., Guimaraes, M., and Santamarina, C., *Micaceous Sands: Microscale mechanisms and macroscale responses.* Journal of Geotechnical and Geoenvironmental Engineering, 2007. 133(9): 1136-1143.

[22]. Murdock, L.J., Brook, K.M., and Dewar, J.D., *Concrete: Materials and Practice*. 6 ed. 1991: Edward Arnold.

[23]. Neville, A.M., *Properties of Concrete*. 4 ed. 1995: Longman Group Ltd.

[24]. Mavko, G. and Nur, A., *Wave attenuation in partially saturated rocks.* Geophysics, 1979. 44: 161-178.

[25]. Palmer, I.D. and Traviolia, M.L., *Attenuation by squirt flow in undersaturated gas sands.* Geophysics, 1980. 45(12): 1780-1792.